Wireless Impedance-Based SHM for Bolted Connections via Multiple PZT-Interfaces

Khac-Duy Nguyen* and Jeong-Tae Kim*[†]

Abstract This study presents a structural health monitoring (SHM) method for bolted connections by using multi-channel wireless impedance sensor nodes and multiple PZT-interfaces. To achieve the objective, the following approaches are implemented. Firstly, a PZT-interface is designed to monitor bolt loosening in bolted connection based on variation of electro-mechanical(EM) impedance signatures. Secondly, a wireless impedance sensor node is designed for autonomous, cost-efficient and multi-channel monitoring. For the sensor platform, Imote2 is selected on the basis of its high operating speed, low power requirement and large storage memory. Finally, the performance of the wireless sensor node and the PZT-interfaces is experimentally evaluated for a bolt-connection model. Damage monitoring method using root mean square deviation(RMSD) index of EM impedance signatures is utilized to estimate the strength of the bolted joint.

Keywords: Electro-Mechanical Impedance, Impedance Sensor Node, Imote2, PZT-Interface, Multiplexer, AD5933

1. Introduction

A complex structure is constructed by assembling many subsystems to become a complete structure. In steel structures such as bridge, pipeline system and tower, bolts are usually used to connect structural members together because of its convenience, time efficient and high reliability. The strength of the connection is guaranteed by axial internal force of bolt. However, as discontinuous parts of structures, bolted connections are influenced by severe repeated loading and various environmental conditions. These conditions may cause decrement of bolt preload or even loosening of bolt. As a result, load carrying capacity of the connection is reduced and the structure could be collapsed. Therefore, structural health monitoring (SHM) on bolted connection becomes a key issue to ensure the safety and serviceability of a structure.

The works on SHM of bolted connections have been carried out by many researchers in global and local SHM ways [1-5,30,31]. The global SHM which usually deals with acceleration-based methods can monitor the structural integrity with several distributed sensors. However, acceleration-based methods are not very sensitive to local incipient damage since these methods employ the low frequency responses which could not cover the change in small region. On the other hand, impedance-based local SHM is found very promising to capture small damage at limited region like bolted connection by using high frequency responses.

Although the impedance-based method could localize damage region and monitor damage severity of bolted connection, which bolts loosened have not been indicated. As a solution for this issue, Mascarenas et al.[6] proposed a

PZT enhanced washer to monitor loosening of individual bolt by examining level of electro-mechanical (EM) impedance at resonance. In our previous study by Park et al.[7], the other type of interface washer was designed to monitor the loss of tendon force of tendon-anchorage connection based on variation of EM impedance. This interface washer was also implemented to bolted connection to monitor loosened bolts [8]. However, for large-scale structure, hundreds of bolts can exist at one bolted connection. Therefore, in order to monitor efficiently the connection, it needs to develop a monitoring system with multiple interface washers.

Besides, developing an efficient wireless SHM system for bolted connection is also important to reduce the cost and time associated with installation and maintenance of conventional SHM. The advantages of wireless sensor networks over the wired SHM system have been discussed by many researchers [9-15]. Therefore, many efforts on developing wireless impedance sensor node(WISN) have been made by Mascarenas et al.[16] and Park et al.[7]. They designed the WISN based on Atmega128 microcontroller which had limited storage memory and low operating speed. Associated with multiple interface washers, it needs to develop a sensor node which has capability to measure EM impedances from multiple PZT sensors. Also, the storage memory must be large enough for multiple sensors monitoring.

The objective of this paper is to address the above-mentioned issues by developing a system of multi-channel wireless impedance sensor nodes and multiple PZT-interfaces for SHM on bolted connection. To achieve the objective, the following approaches are implemented. Firstly, a PZT-interface is designed to monitor bolt loosening in bolted connection based on variation of electro-mechanical (EM) impedance signatures. Secondly, a wireless impedance sensor node is

designed for autonomous, cost-efficient and multi-channel monitoring. For the sensor platform, Imote2 is selected on the basis of its high operating speed, low power requirement and large storage memory. Finally, the performance of the wireless sensor node and the PZT-interfaces is experimentally evaluated for a bolt-connection model. Damage monitoring method using root mean square deviation (RMSD) index of EM impedance signatures is utilized to estimate the strength of the bolted joint.

2. Impedance-Based Method

The impedance-based method is based on the coupling of mechanical and electrical features[17]. In this method, a piezoelectric patch is usually surface-bonded to a host structure. The electrical responses of piezoelectric materials are partly controlled by mechanical behavior of host structure. As shown in Fig. 1, the interaction between the piezoelectric patch and the host structure is conceptually explained as an idealized 1-D electro-mechanical relation. The host structure is described as the effects of mass, stiffness, damping, and boundary condition. The PZT patch is modeled as a short circuit powered by a harmonic voltage or current. The EM impedance $Z(\omega)$ which is generated from the PZT patch is a combined function of the mechanical impedance of the host structure, $Z_s(\omega)$, and that of the piezoelectric patch, $Z_a(\omega)$, as follows:

$$Z(\omega) = \left\{ j\omega \frac{wl}{t_c} \left[\left(\hat{\varepsilon}_{33}^T - d_{3x}^2 \hat{Y}_{xx}^E \right) + \frac{Z_a(\omega)}{Z_a(\omega) + Z_s(\omega)} d_{3x}^2 \hat{Y}_{xx}^E \left(\frac{\tan kl}{kl} \right) \right] \right\}^{-1}$$

(1)

where, $\hat{Y}_{xx}^E = (1 + j\eta)Y_{xx}^E$ is the complex Young's modulus of the PZT patch at zero electric field; $\hat{\varepsilon}_{xx}^T = (1 - j\delta)\varepsilon_{xx}^T$ is the complex dielectric constant at zero stress; d_{3x} is the piezoelectric coupling constant in x-direction at zero stress; $k = \omega \sqrt{\rho / \hat{Y}_{xx}^E}$ is the wave number where ρ is

the mass density of the PZT patch; and w, l, and t_c are the width, length, and thickness of the piezoelectric transducer, respectively. The parameters η and δ are structural damping loss factor and dielectric loss factor of piezoelectric material, respectively. In eqn. (1), the mechanical impedance of the host structure Z_s (ω) is the ratio of PZT force to structural velocity at PZT location, as follows:

$$Z_s(\omega) = \frac{f_{PZT}}{\dot{x}_{PZT}} = \frac{F_{PZT}e^{i\omega t}}{\dot{x}_{PZT}} \qquad (2)$$

If the structure is considered as a system of single degree of freedom, the mechanical impedance of the host structure can be expressed as:

$$Z_s(\omega) = m\omega j + c - \frac{k}{\omega}j \qquad (3)$$

Equation (3) shows that the mechanical impedance of the host structure is a function of mass (m), damping (c) and stiffness (k). Therefore, any change in dynamic characteristics of the structure could be represented in the change in EM impedance.
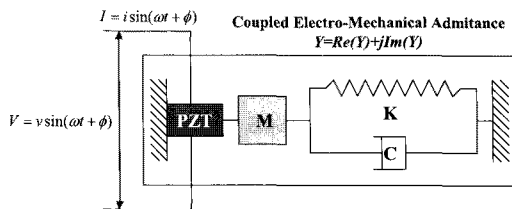

Fig.1   1-D electro-mechanical interaction of PZT sensor and its host structure
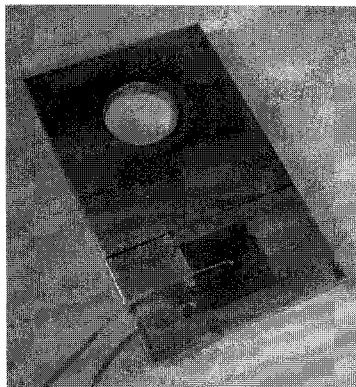
3. PZT-Interface for Loose Bolt Monitoring

Even though the impedance-based method shows the excellent performance in local SHM in many various aspects, this method still has some limitations for civil engineering applications. The drawbacks can be pointed out as follows:

(1) In order to measure EM impedance, a bulky impedance analyzer is usually used.

However, this device is not designed to work out of laboratory. Moreover, the cost associated with the wired system using this device is very high. Efforts to overcome these disadvantages have been carried out by adopting wireless impedance device[7, 16]. In order to apply the new approach, however, the measurable frequency range 10 kHz - 100 kHz of the wireless sensors should be dealt appropriately for impedance measurement as well as feature extraction. This frequency range is relatively low compared with that of the impedance analyzer. The low frequency may interfere with wide applications in real-scale structures. For example, in the previous study by Kim et al.[18], the frequency range sensitive to prestressed force loss of cable-anchorage connection was found at 880 kHz - 980 kHz.

(2) In order to employ the impedance-based method for damage detection, the frequency range which is sensitive to damage has to be identified. Generally, the effective frequency range is various depending on target structures and usually determined by trial and error. This causes difficulty when applying the impedance- based method to real structure since the effective frequency range is almost unknown and may take much effort to obtain it by trial and error.

The above-mentioned limitations could be overcome for SHM on bolted connections by employing a PZT-interface equipped with a PZT patch as designed in Fig. 2. The PZT-interface is made of aluminum for low mechanical impedance, and its entire dimension is 100×60×5 mm. The PZT patch is PZT-5A type (Piezo Systems[19]) and its size is selected as 20×20×0.5 mm. Geometries of the interface washer and the PZT patch are described in detail in Fig. 2(b). The PZT patch is surface-bonded on the interface washer at

(a) PZT-interface
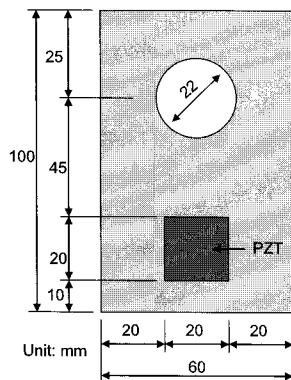
(b) Geometry of PZT-interface
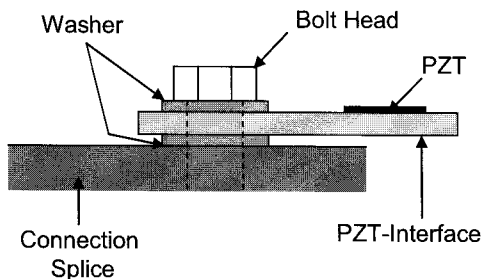
Fig. 2   PZT-interface for loose bolt monitoring

Fig. 3   Schematic of PZT-interface and connection splice

30 mm from the left edge and 20 mm from the bottom edge of the interface washer. A hole with same size as inner diameter of bolt washer (22 mm) is drilled to allow a bolt get through the interface.

Fig. 3 shows how the interface can be utilized for monitoring preload of bolted joint. As shown in Fig. 3, the PZT-interface is installed between two bolt washers and clamped by bolt head and connection splice. The bolt washers are utilized to keep geometrical boundary of the PZT-interface stable. Also, by installing between two washers, the PZT-interface behaves like a cantilever plate with imperfectly fixed edge. The imperfectly fixed boundary condition of the PZT-interface can be expressed as effects of damping and stiffness. It was previously shown that values of boundary damping and stiffness depend on contact pressure or preload level of bolted joints[20,21]. As the change in mechanical impedance of structure, the variation of damping and stiffness at the fixed edge can be represented by the change in EM impedance measurements from the PZT patch. It is worth noting that the natural frequencies of the cantilever-like PZT-interface are usually smaller than 100 kHz which is appropriate for wireless impedance-based SHM. Furthermore, we can adjust the resonance frequencies of interest by designing dimensions and materials of the interface.

4. Design of Wireless Multi-Channel Impedance Sensor Node

4.1 Hardware Design of Multi-Channel Impedance Sensor Node

Recently, the Imote2 sensor platform has shown the excellent performance for wireless SHM operation. The large memory and high operating speed of Imote2 allows it enable for advanced complicated smart SHM techniques. SHM-A which is developed by UIUC[22,23] is a typical example of sensor board based on Imote2 platform. The combined Imote2/SHM-A sensor node has good capability to measure three-dimensional acceleration which can be used for vibration-based global SHM.

As summarized in Table 1, the Imote2 has the high performance microcontroller and the

large amount of data repository as compared to a smart sensor node(SSN) by Park et al.[7]. Firstly, the main board of the Imote2 incorporates a low-power X-scale process, PXA27x, and a wireless radio, CC2420. The microcontroller PXA27x runs for multiple tasks which include operation schedule, system control, and radio transmission. It allows double-point precision valuables using 8 bytes. Note that a microcontroller ATmega128 used by Lynch et al.[12] and Park et al.[7] allows single precision floating point format using 4 bytes. Secondly, the Imote2 has 256 kB of integrated SRAM, 32 MB of external SDRAM, and 32 MB of program flash memory. The memory repository guarantees to store large amount of data measured from many PZT sensors. Thirdly, although the Imote2 consumes more power in high-speed mode and the embedded wireless radio has short transmitting distance, the data processing speed of the Imote2 is faster enough to provide good computational capability and the transmitting distance can be expanded up to 125 m by using an external antenna. Based on the above-mentioned performances, the Imote2 sensor platform is selected for the smart impedance-based SHM system.

In this study, we propose a multi-channel impedance sensor board so called SSeL-I16 based on Imote2 sensor platform. The combined Imote2/SSeL-I16 sensor node has the capability to measure EM impedances from multiple (up to 16) PZT patches. The design schematic of the Imote2/SSeL-I16 sensor node is given in Fig. 4. The Imote2 platform is utilized for controlling impedance measurement, and for wireless communication by the on-board microcontroller PXA27x and wireless radio CC2420. The core component of the sensor node is the AD5933 impedance chip. The AD5933 was first used for measuring EM impedance signatures by Mascarenas et al[16]. This impedance chip has the capability to measure electric impedance up to 100 kHz. The AD5933 impedance chip has the following embedded multi-functional circuits: function generator, digital-to-analog(D/A) converter, current-to-voltage amplifier, anti-aliasing filter, A/D converter, and discrete Fourier
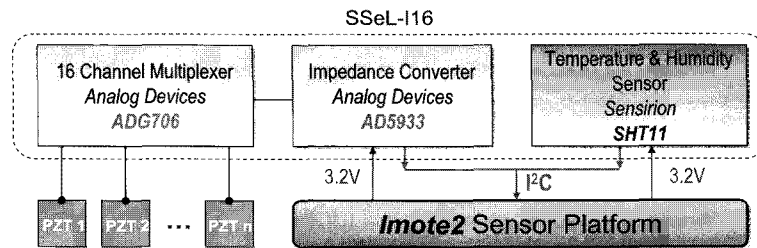

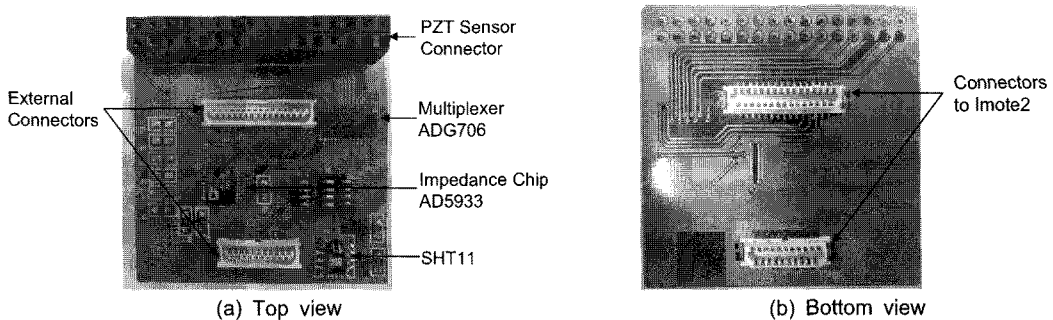Fig. 4 Design schematic of multi-channel impedance sensor nodes

(a) Top view   (b) Bottom view

Fig. 5 Components of impedance sensor board SSeL-I16

Table 1 Feature comparison of Imote2 and SSN

Feature	Imote2 [22]	SSN by Park et al. [7]
Clock speed (MHz)	13-416	16
Active power (mW)	44 at 13 MHz 570 at 416 MHz	23 at 8 MHz 46 at 16 MHz
Program flash (bytes)	32 M	128 K
RAM	256 K + 32 M external	4 K + 32 K
Radio Frequency (MHz)	2400	2400
Data rate (kbps)	250	250
Outdoor range (m)	30 (125 with antenna)	100
Power of Radio (mW)	52 when transmitting 59 when receiving 0.06 when powered-down	149 when transmitting 165 when receiving 0.03 when powered-down

Table 2 Power consumption by Imote2/SSeL-I16

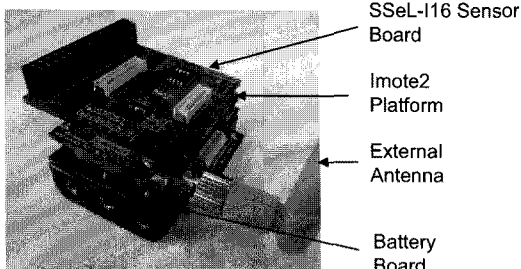| Operating Task	Power draw (mW)
Measuring	248
Receiving	216
Transmitting	212

Fig. 6 Prototype of Imote2/SSeL-I16 unit

transform(DFT) analyzer. The AD5933 outputs real and imaginary values of impedance for a target frequency of interest and transmits the values into a microcontroller. The AD5933 interacts with an ADG706 multiplexer to allow monitoring EM impedance from up to sixteen PZT sensors by a single sensor node. The ADG706 multiplexer has the role as a digital switch to select specified channel to be measured by the AD5933. An SHT11 sensor is also integrated into SSeL-I16 board to monitor temperature and humidity of environment.

The components of SSeL-I16 board are pointed out in Fig. 5. As shown in Fig. 5, the SSeL-I16 board connects to Imote2 through 31-pin and 21-pin connectors at the bottom side. It also allows other external devices to connect to the Imote2 by returning connectors at the top side. A photo of the Imote2/SSeL-I16 sensor node is shown in Fig. 6 with three layers: a battery board (IBB2400), the Imote2 sensor platform (IPR2400) and the SSeL-I16 sensor board. The power drawn by the Imote2/SSeL-I16 sensor node is included in Table 2. The power for measuring, receiving, and transmitting is 248 mW, 216 mW and 212 mW, respectively. Note that, power for receiving and transmitting is much larger than that specified in Table 1 since the sensor node is integrated with an external antenna.

4.2 Software Design of Multi-Channel Impedance Sensor Node

The operating software for the Imote2/SSeL-I16 is programmed on TinyOS platform. TinyOS is a free and open source component-based operating system. It has a huge library of basic components which meet most of user's demands. Especially, TinyOS is very strong for designing wireless sensor networks.

The wireless monitoring system is illustrated in Fig. 7. The system starts when the user makes a request of EM impedance to remote node from local node. Frequency range and channels of sensor are transmitted to local node
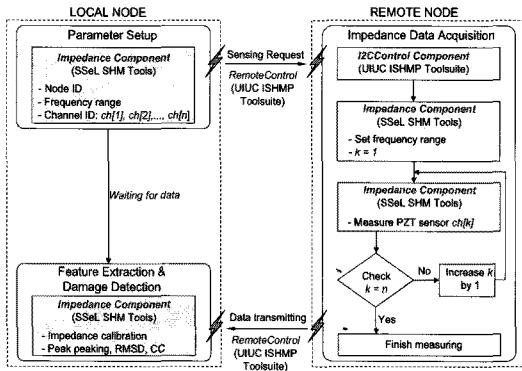
Fig. 7 Schematic of embedded software

through "RemoteControl" component. After receiving request, the remote node measures real and imaginary parts of EM impedance from the defined channels, sequentially. When EM impedance signatures of all defined channels are completely measured, data are transmitted to the local node. At the local node, the raw EM impedance signatures are calibrated and processed to feature extraction and damage monitoring using resonance frequency, RMSD or correlation coefficient(CC). It is worth noting that, the "RemoteControl" component for wireless transmitting and the "I2CControl" component for TWI protocol controlling are provided from ISHMP Services Toolsuite[25]; and the "Impedance" component is newly developed in SSeL SHM Tools by our research group.

4.3 Measurement Evaluation of Multi-Channel Impedance Sensor Node

Before adopting the Imote2/SSeL-I16 to a wireless SHM system, it is essential to evaluate measurement performance of the sensor node. Thus, EM impedances of the PZT-interface with free boundary condition measured by a commercial impedance analyzer HIOKI 3532-50 and by the Imote2/SSeL-I16 are compared each other. According to the datasheet of the AD5933, the recommend measurable impedance

is larger than 1 kΩ. The calibration method performed in the datasheet using a know resistance is also suitable for the impedance larger than 1 kΩ. In this study, EM impedance of the PZT patch was found smaller than 1 kΩ after 15 kHz and it decreased gradually with the frequency range. Therefore, the raw measurement by the Imote2/SSeL-I16 was calibrated with EM impedance by a commercial impedance analyzer HIOKI 3532-50 for the PZT-interface with free-free boundary condition. The impedance amplitude by the Imote2/SSeL-I16 was calibrated with a linear function of gain factor. Phase difference between impedance measurements by the sensor node and the impedance analyzer was also adjusted by another linear function. Fig. 8 illustrates EM impedance signatures in frequency range 10 kH – 50 kHz with 501 points by the
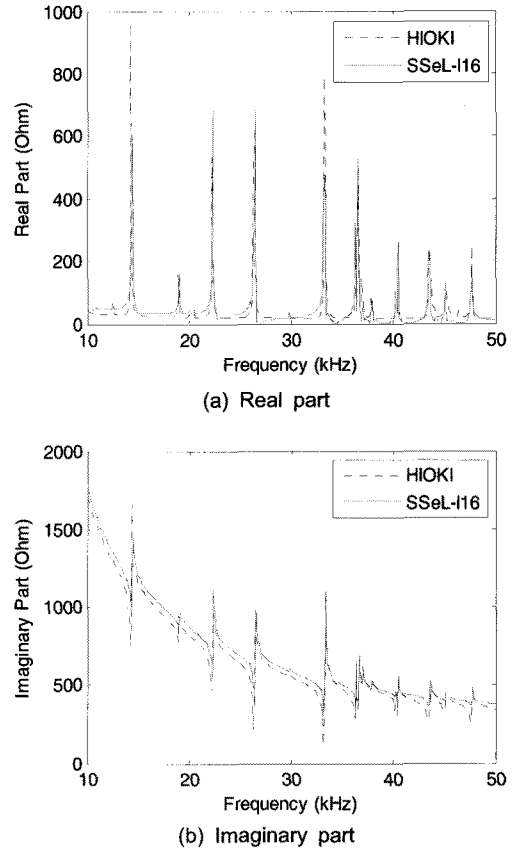

(a) Real part

(b) Imaginary part

Fig. 8 Impedance measurements by wired and wireless systems

Imtote2/SSeL-I16 and the impedance analyzer. As shown in Fig. 8, both real part and imaginary part of impedance by the sensor node show the good matching with those by the wired commercial system. Note that, the real part of impedance contains much more information of structural behaviors than imaginary part. Meanwhile, the imaginary part is useful for monitoring sensor's health status and bonding condition[26]. It is also worth noting that the HIOKI 3532-50 is very costly (US$ 10,000) compared with the Imote2/SSeL-I16 (US$ 350).

5. Loose Bolt Monitoring for Bolted Connection

For loose bolt detection with PZT-interfaces, it is convenient for monitoring by establishing a unique baseline. The PZT-interfaces, therefore, should be examined on repeatability of EM behavior. Fig. 9 shows EM impedance signatures of four PZT-interfaces with free boundary condition measured by the Imote2/SSeL-I16. There is slight difference in impedance amplitude. This may be caused by inhomogeneity in bonding condition and in geometries of the PZT patches. However, the resonance frequencies of EM impedances are well repeated. The

similarity of EM impedances of the four PZT-interfaces guarantees the similar behavior of the PZT-interfaces due to bolt preload.

A steel girder with bolted connection as shown in Fig. 10 was utilized to evaluate performance of the Imote2/SSeL-I16 and multiple PZT-interfaces. The girder was constructed from two single H-shaped beams (H – 200×180×8×100) by connection splice plates and 2-cm-diameter bolts at two flanges. The girder had total length 4.14 m and was hung on by two strings at two ends of the girder. At the bolted connection, we put a PCB393B04 accelerometer for acceleration-based monitoring. The impact excitation was applied at one-fourth length of the girder distant from the left ends.
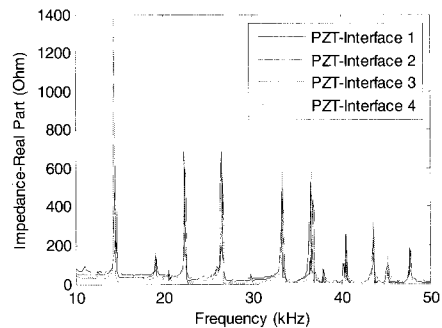

Fig. 9 Impedance measurements from four PZT-interfaces with free boundary condition
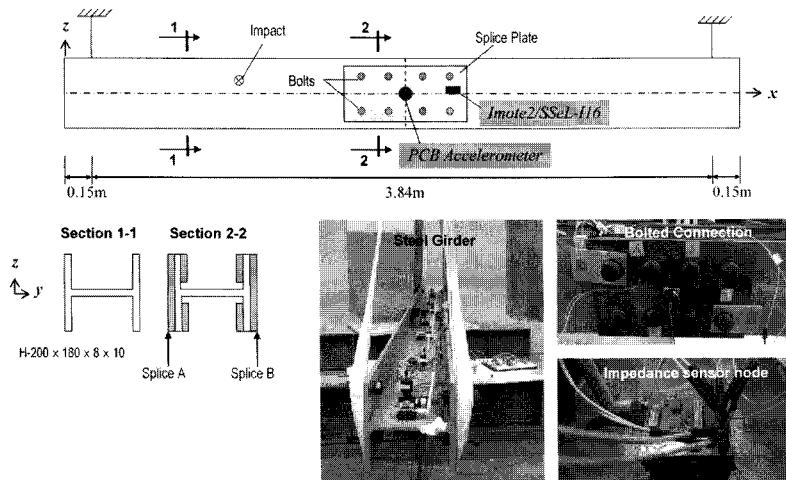

Fig. 10 Experimental setup for a lab-scale bolt-connected steel girder

Table 3 Damage scenarios on girder's bolt-connection

Case	Description	Loosened Bolts
Intact	All bolts fastened to 160 N.m	None
D1	Bolt 1 loosened by 40 N.m	1
D2	Bolt 2 loosened by 40 N.m	1, 2
D3	Bolts 1&2 refastened, Bolt 5 loosened by 40 N.m	5
D4	Bolt 6 loosened by 40 N.m	5,6
D5	Bolt 3 loosened by 40 N.m	5,6,3
D6	Bolt 4 loosened by 40 N.m	5,6,3,4
D7	Bolts 5, 6, 3, 4 refastened	None

(a) Splice A   (b) Splice B
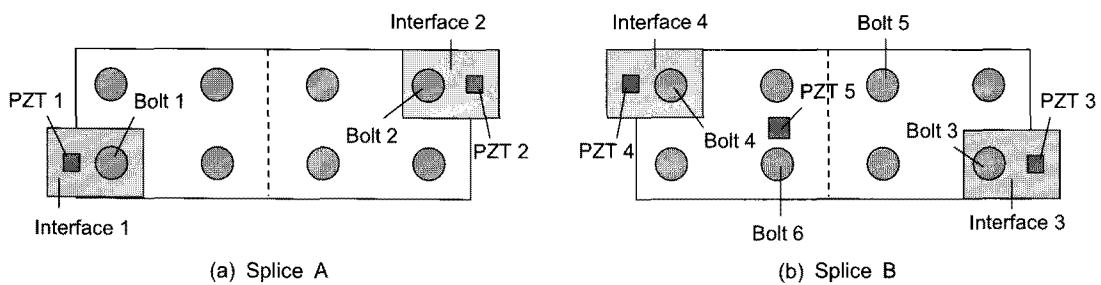
Fig. 11 Arrangement of PZT-interfaces at two splices

Also, four PZT-interfaces were installed to four bolts at two connection splices as shown in Fig. 11. The PZT-interfaces were marked as Interface 1-4 correspondent to Bolt 1-4. Beside the PZT patches (PZT 1-4) bonded on the four interfaces, another PZT patch with the same size (PZT 5) was bonded directly on a connection splice to monitor bolt loosening in a conventional way. A wireless impedance sensor node (Imote2/ SSeL-I16) was placed at the bolted connection as shown in Fig. 10. Upper and lower surfaces of five PZT patches were linked to the connector of SSeL-I16 through five double electrical wires. A base station which included an Imote2 associated with an interfacial board IIB2400 and a computer was placed at 5 m distant from the steel girder. The IIB2400 provides two ports from Imote2 to the computer, one for sending command and receiving debug messages from remote node, and one for communicating data. A command-line interface, Cygwin OS[27], was utilized to operate the

wireless system.

The damage scenarios with regarding bolt loosening are outlined in Table 3. A torque wrench was used to fasten the bolts and to control the bolt torques as well. Firstly, all bolts were fastened to 160 N.m, which was considered as healthy condition. Then, Bolt 1 and Bolt 2 were loosened by 40 N.m in damage cases D1 and D2, sequentially. Subsequently, Bolt 5 was loosened by 40 N.m after refastening Bolt 1 and Bolt 2 to 160 N.m. Then Bolt 6, Bolt 3 and Bolt 4 were loosened by 40 N.m sequentially in the next scenarios. Finally, all bolts were refastened to healthy condition. The loosened bolts in each scenario are clearly summarized in the third column of Table 3.

The acceleration-based monitoring results are illustrated in Figs. 12 and 13. Fig. 12 shows the time history response followed by the power spectral density(PSD) of acceleration. The occurrence of damage was monitored by using correlation coefficient(CC) of PSD[28]. The CC

of PSD is expressed as follows:

$$\rho_{XY} = \frac{E[S_{xx}(f)S_{yy}(f)] - E[S_{xx}(f)]E[S_{yy}(f)]}{\sigma_{Sxx}\sigma_{Syy}} \quad (4)$$

where $E[\cdot]$ is the expectation operator, $S_{xx}(f)$ and $S_{yy}(f)$ are power spectral densities at undamaged and damaged states, respectively and σ_{Sxx} and σ_{Syy} are the standard deviations of PSDs of acceleration signals measured before and after damaging episode, respectively. Basically, if there is no damage in the structure, the PSD of acceleration is remained unchanged, and CC has value as 1. If damage occurs in the structure, it will cause the changes in acceleration responses and CC value will be decreased, as a result. Generally, the amount of CC decrement is directly proportional to the severity of the damage but inversely proportional to the distance from the damage to accelerometer. As shown in Fig. 13, value of CC decreases with the severity of damage. However, the reason of damage (i.e., crack, bolt loosening) or which bolts are loosened can not be clearly indicated by this index.

Fig. 14 illustrates EM impedance signatures of Interface 4 for the healthy state and four damaged states (i.e. cases D3-D6). The impedance signatures are significantly changed when Bolt 4 correspondent to Interface 4 is loosened. Resonance frequencies tend to shift left which indicates the decrement of modal stiffness of the PZT-interface. Also, the variation of resonance impedances represents the change in modal damping of the PZT-interface. It is worth noting that there are small changes in EM impedance around 12 kHz and 37 kHz. This implies not all modal parameters of the PZT-interface are sensitive to bolt loosening. It is also worth noting that the loosening of other bolts almost does not affect to the EM impedance of PZT 4. Thus, the PZT-interface is efficient to monitor itself bolt-loosening.
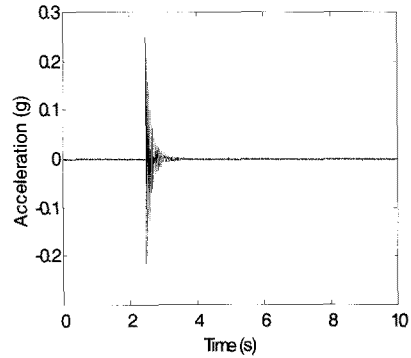
(a) Time history acceleration
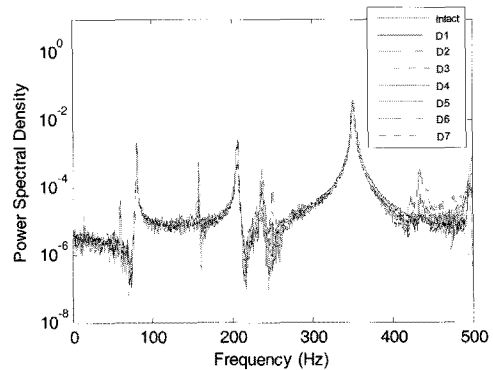
(b) Power spectral density of acceleration
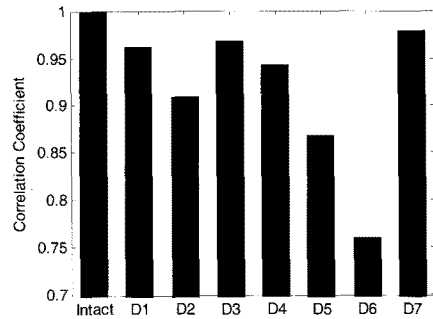Fig. 12 Acceleration responses from PCB sensor

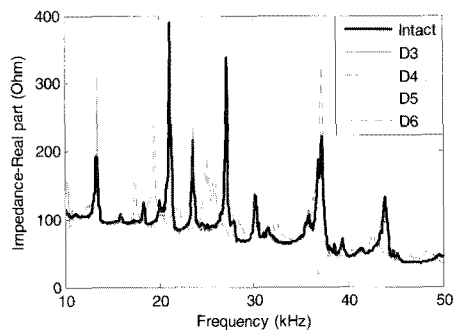Fig. 13 Correlation coefficients of PSDs

Fig. 14 Impedance signatures from PZT 4

On the other hand, by examining EM impedance from PZT 5 on the connection splice (Fig. 15), it is difficult to capture the change in the impedance signatures of PZT 5 due to damages. The peaks are very small, that could not reflect clearly vibration responses of the structure against PZT force. Generally, EM impedance is more sensitive to damage in resonance range than in non-resonance range[29]. The EM impedance in resonance range performs resonance responses of structure against the force induced from the PZT patch. In this case, PZT 5 is bonded to the connection splice which is very rigid. The sensitive frequency range may be found at higher than 100 kHz which exceed the measurement capability of the AD5933 chip.

In order to quantify the change in EM impedance due to damage, RMSD index is utilized. The RMSD index is calculated by following equation:

$$RMSD = \sqrt{\frac{\sum_{i=1}^{n}\left[Re(Z^{*}(\omega_{i})) - Re(Z(\omega_{i}))\right]^{2}}{\sum_{i=1}^{n}\left[Re(Z(\omega_{i}))\right]^{2}}} \qquad (5)$$

where $Re(Z(\omega_{i}))$ and $Re(Z^{*}(\omega_{i}))$ are the real parts of the impedance signatures of the ith frequency measured before and after damage occurrence, respectively. Also, n signifies the number of frequency points in the sweep band.

Fig. 16 shows the RMSD results of EM impedance signatures from five PZT patches. The loosening of Bolt 1-4 can be clearly indicated by the correspondent PZT-interfaces. Meanwhile, PZT 5 on the connection splice can not indicate any damage in the connection, even thought four bolts at the same splice were loosened. This implies the changes of structural impedance obtained from PZT 5 are very small compared with coupled EM impedance. It is worth noting that the loosening of Bolt 5 and Bolt 6 slightly influences to impedance
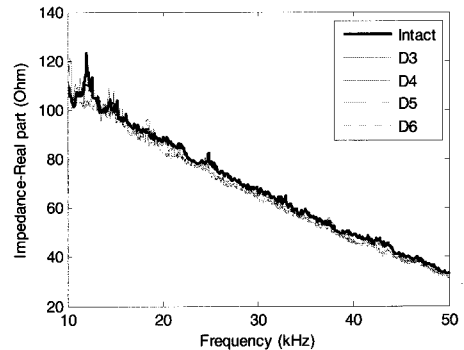

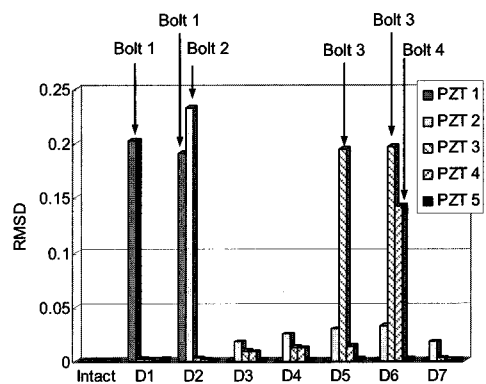Fig. 15 Impedance signatures from PZT 5

Fig. 16 RMSD index of EM impedances

signatures of the PZT-interfaces. It may be explained by the redistribution of preload of bolt group after loosening any of them.

6. Conclusions

In this study a SHM method for bolted connections by using multi-channel wireless impedance sensor nodes and multiple PZT-interfaces was presented. Firstly, a PZT-interface was designed to monitor bolt loosening in bolted connection based on variation of EM impedance signatures. Secondly, wireless impedance sensor node based on the Imote2 platform was designed for autonomous, cost-efficient and multi-channel monitoring. The impedance sensor node was integrated with an AD5933 impedance chip for EM impedance measurement and an ADG706 multiplexer for

multi-channel measurement. Finally, performance of the wireless sensor nodes and multiple PZT-interfaces was experimentally evaluated for a bolted connection model.

From the experimental results, the following conclusions have been made from this study:

(1) The PZT-interface is efficient to monitor bolt loosening by using low frequency (less than 100 kHz) EM impedance.

(2) The wireless impedance sensor node Imote2/SSeL-I16 can measure EM impedance very precisely compared with the bulky, expensive commercial impedance analyzer.

(3) The wireless monitoring system of Imote2/SSeL-I16 sensor nodes with multiple PZT-interfaces shows the excellent performance to indicate loosened bolts in bolted connection.

Acknowledgements

References

[1] H. F. Lam, J. M. Ko and C. W. Wong, "Localization of damaged structural connections based on experimental modal and sensitivity analysis," *Journal of Sound and Vibration*, Vol. 210, No. 1, pp. 91-115 (1998)

[2] C. B. Yun, J. H. Yi and E. Y. Bahng, "Joint damage assessment of framed structures using neural networks technique," *Engineering Structures*, Vol. 23, No. 5, pp. 425-435 (2001)

[3] J. T. Kim, W. B. Na, J. H. Park and D. S. Hong, "Hybrid health monitoring of structural joints using modal parameters and EMI signatures," *Proceeding of SPIE*, San Diego, USA, Vol. 6171 (2006)

[4] T. R. Fasel, H. Sohn, G. Park and C. R. Farrar, "Active sensing using impedance-based ARX models and extreme value statistics for damage detection," *Earthquake Engineering and Structural Dynamics*, Vol. 34, No. 7, pp. 763-785 (2005)

[5] S. Park, C. B. Yun and Y. Roh, "PZT-induced lamb waves and pattern recognitions for on-line health monitoring of joint steel plates," *Proceeding of SPIE*, San Diego, USA, Vol. 5765, pp. 364-375 (2005)

[6] D. L. Mascarenas, "Development of an impedance-based wireless sensor node for monitoring of bolted joint preload," *MS Thesis*, Department of Structural Engineering, University of California, San Diego (2006)

[7] J. H. Park, J. T. Kim, D. S. Hong, D. Mascarenas and J. P. Lynch, "Autonomous smart sensor nodes for global and local damage detection of prestressed concrete bridges based on accelerations and impedance measurements," *Smart Structures and Systems*, Vol. 6, pp. 711-730 (2010)

[8] J. H. Park, D. D. Ho, K. D. Nguyen and J. T. Kim, "Multi-scale hybrid sensor nodes for acceleration-impedance monitoring for steel structural connections," *Proceeding of SPIE*, San Diego (2011)

[9] E. G. Straser and A. S. Kiremidjian, A Modular, "Wireless damage monitoring system for structure," *Technical Report 128*, John A. Blume Earthquake Engineering Center, Stanford University, Stanford, CA (1998)

[10] B. F. Spencer, M. E. Ruiz-Sandoval and N. Kurata, "Smart sensing technology: opportunities and challenges," *Structural Control and Health Monitoring*, Vol. 11, pp. 349-368 (2004)

[11] N. Kurata, B. F. Spencer and M. Ruiz-Sandoval, "Risk monitoring of buildings with wireless sensor networks," *Structural Control and Health Monitoring*, Vol. 12, pp. 315-327 (2005)

[12] J. P. Lynch and K. Loh, "A summary review of wireless sensors and sensor networks for structural health monitoring," *Shock and Vibration Digest*, Vol. 38, No. 2, pp. 91-128 (2006)

[13] T. Nagayama, S. H. Sim, Y. Miyamori and B. F. Spencer, "Issues in structural health monitoring employing smart sensors," *Smart Structures and Systems*, Vol. 3, No. 3, pp. 299-320 (2007)

[14] V. Krishnamurthy, K. Fowler and E. Sazonov, "The effect of time synchronization of wireless sensors on the modal analysis of structures," *Smart Materials and Structures*, Vol. 17, No. 5, pp. 1-13 (2008)

[15] D. Dhital, C. C. Chia, J. R. Lee and C. Y. Park, "Review of radio frequency identification and wireless technology for structural health monitoring," *Journal of the Korean Society for Nondestructive Testing*, Vol. 30, No. 3, pp. 244-256 (2010)

[16] D. L. Mascarenas, M. D. Todd, G. Park, and C. R. Farrar, "Development of an impedance-based wireless sensor node for structural health monitoring," *Smart Materials and Structures*, Vol. 16, No. 6, pp. 2137-2145 (2007)

[17] C. Liang, F. P. Sun and C. A. Rogers, "Electro-mechanical impedance modeling of active material systems," *Smart Materials and Structures*, Vol. 5, No. 2, pp. 171-186 (1996)

[18] J. T. Kim, J. H. Park, D. S. Hong and W. S. Park, "Hybrid health monitoring of prestressed concrete girder bridges by sequential vibration-impedance approaches," *Engineering Structures*, Vol. 32, pp.115-12 (2010)

[19] Piezo Systems, http://piezo.com

[20] S. Ritdumrongkul, M. Abe, Y. Fujino and T. Miyashita, "Quantitative health monitoring of bolted joints using a piezoceramic actuator-sensor," *Smart Materials and Structures*, Vol. 13, pp. 20-29 (2004)

[21] M. Yoshimura and K. Okushima, "Measurement of dynamic rigidity and damping property for simplified joint models and simulation by computer," *CIRP Annals*, pp. 193-198 (1997)

[22] J. A. Rice and B. F. Spencer, "Structural health monitoring sensor development for the Imote2 platform," *Proc. of SPIE*, Vol. 6932, San Diego (2008)

[23] J. A. Rice, K. Mechitov, S. H. Sim, T. Nakayama, S. Jang, R. Kim, B. F. Spencer, G. Agha and Y. Fujino, "Flexible smart sensor framework for autonomous structural health monitoring," *Smart Structures and Systems*, Vol. 6, No. 5, pp. 423-438 (2010)

[24] Memsic Co., "Datasheet of ISM400," http://www.memsic.com

[25] Illinois Structural Health Monitoring Project, http://shm.cs.uiuc.edu (2010)

[26] T. G. Overly, G. Park, K. M. Farinholt and C. R. Farrar, "Piezoelectric active-sensor diagnostics and validation using instantaneous baseline data," *IEEE Sensors Journal*, Vol. 9, No. 11, pp. 1414-1421 (2009)

[27] Cygwin OS, http://cygwin.com/

[28] J. H. Park, D. S. Hong, J. T. Kim, M. D. Todd and D. Mascarenas, "Development of smart sensor node for hybrid health monitoring on PSC girders," *Proceeding of SPIE*, San Diego, USA, Vol. 6932 (2008)

[29] F. P. Sun, Z. Chaudry, C. A. Rogers, M. Majmundar and C. Liang, "Automated

real-time structure health monitoring via signature pattern recognition," *Proceeding of SPIE*, San Diego, USA, Vol. 2443 (1995)

[30] S. Park, C. B. Yun and D. J. Inman, "Remote impedance-based loose bolt inspection using a radio-frequency active sensing node," *Journal of the Korean Society for Nondestructive Testing*, Vol. 27, No. 3, pp. 217-223 (2007)

[31] H. H. Chun, T. H. Lee, K. Y. Jhang and N. Kim, "Estimation of the axial stress in high-tension bolt by acoustoelastic method," *Journal of the Korean Society for Nondestructive Testing*, Vol. 26, No. 5, pp. 285-290 (2006)